Electronic Supplementary Material (ESI) for Chemical Communications

Combining piracetam and lithium salts: Ionic co-cocrystals and co-drugs?

Dario Braga, Fabrizia Grepioni,*[a] Lucia Maini,*[a] Davide Capucci, Saverio Nanna, Johan Wouters, Luc Aerts and Luc Quéré

Electronic Supplementary Information
(10 pages)

EXPERIMENTAL

All reagents and solvents were purchased from Sigma-Aldrich and used without further purification.

Solid-state synthesis

PIR·LiCl·2H$_2$O and PIR·LiBr·2H$_2$O. PIR (14.2 mg, 1 mmol) and LiX (X = Cl, Br) (LiCl 4.2 mg, LiBr, 8.7 mg, 1 mmol) were manually kneaded in an agate mortar for 5 minutes to help in obtaining the product quantitatively; no solvent was necessary in the reaction, due to the hygroscopicity of LiX.

Solution synthesis

PIR·LiCl·2H$_2$O and PIR·LiBr·2H$_2$O were obtained by dissolution of PIR (14.2 mg,1 mmol) and LiX (X = Cl, Br) (LiCl 4.2 mg, LiBr, 8.7 mg, 1 mmol) in 10 mL of water; the solution was left to evaporate at room temperature and crystals suitable for X-ray single crystal diffraction were obtained.

Thermogravimetric analysis (TGA) . TGA measurements were performed using a Perkin Elmer TGA7 in the temperature range 30-550 °C under N_2 gas flow; heating was carried out at 5 °C min^{-1}.

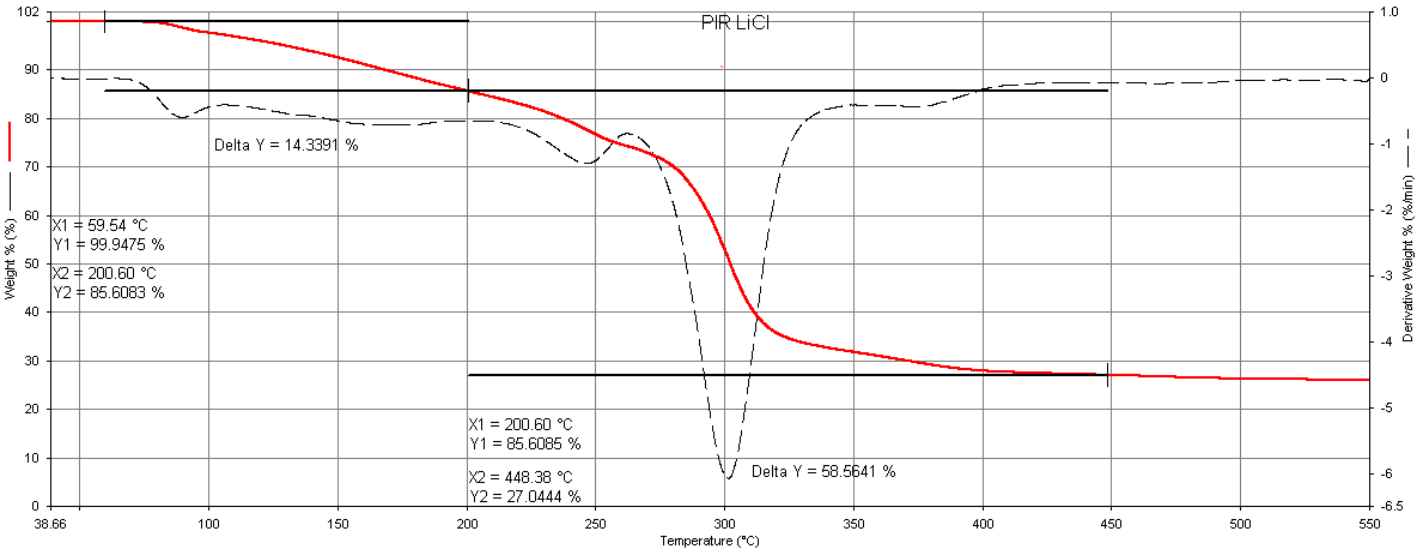

ESI-Fig.1. TGA trace for PIR·LiCl·2H$_2$O

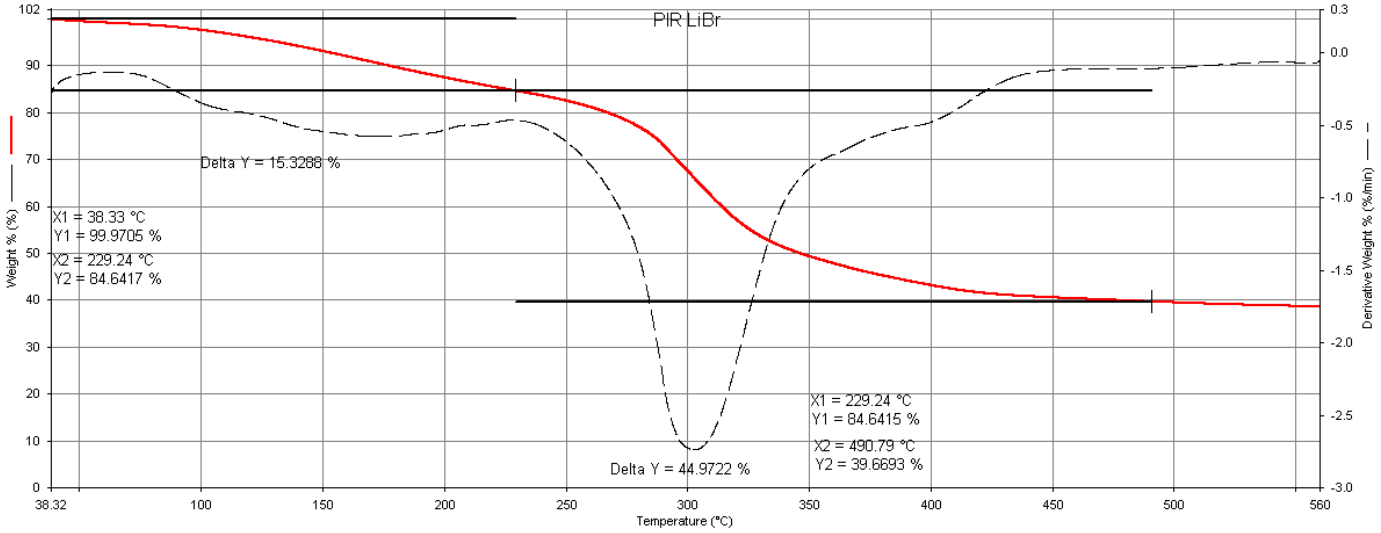

ESI-Fig.2. TGA trace for PIR·LiBr·2H_2O

Differential Scanning Calorimetry (DSC): DSC thermograms were recorded on a Perkin Elmer Diamond equipped with a model ULSP90 intracooler. The samples (3-5 mg, obtained via crystallization) were placed in open or sealed Al-pans. Temperature and enthalpy calibrations were performed using high purity standards (n-decane, benzene and indium). All measurements were conducted in the range 40-160 °C at a heating rate of 5 °C/min.

Measurements in open pan were done in order to follow the dehydration process; in alla cases, though, this was only partially achieved, and melting of the hydrated phase was invariably observed. For this reason hot stage microscopy was employed to better understand the VT-XRPD behavior. In the case of PIR·LiBr·2H_2O, though, it was not possible to observe (even via HSM) formation of the anhydrous phase. Measurements in sealed pan, on the other hand, allowed to accurately determing the congruent melting point of the hydrated forms.

A word of caution: care should be taken in comparing, for the same thermal event, temperatures measured via DSC, TGA, XRPD and HSM, as they can differ, due to the different experimental conditions and different sample amounts.

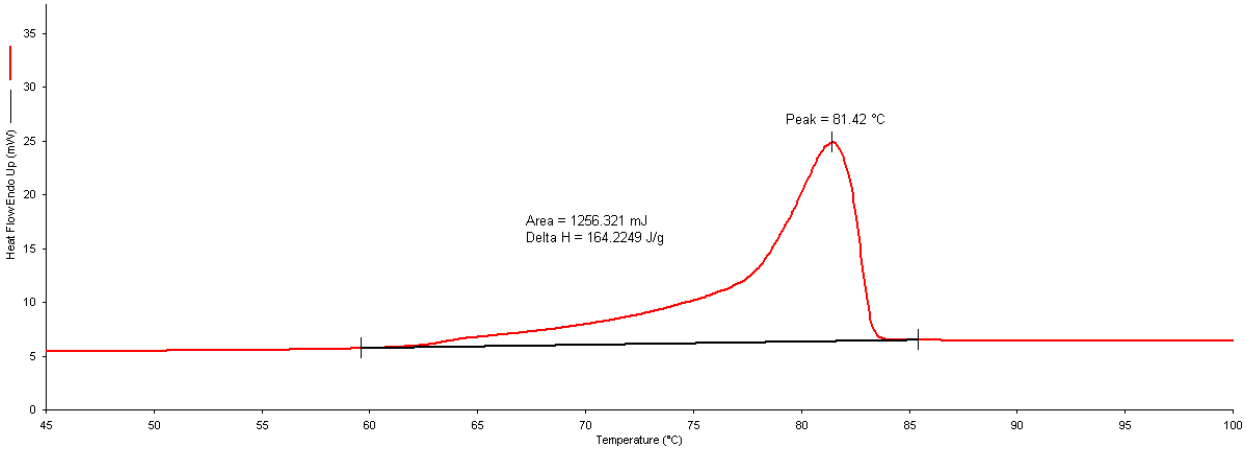

ESI-Fig.3. DSC curve for PIR·LiCl·2H_2O in open pan.

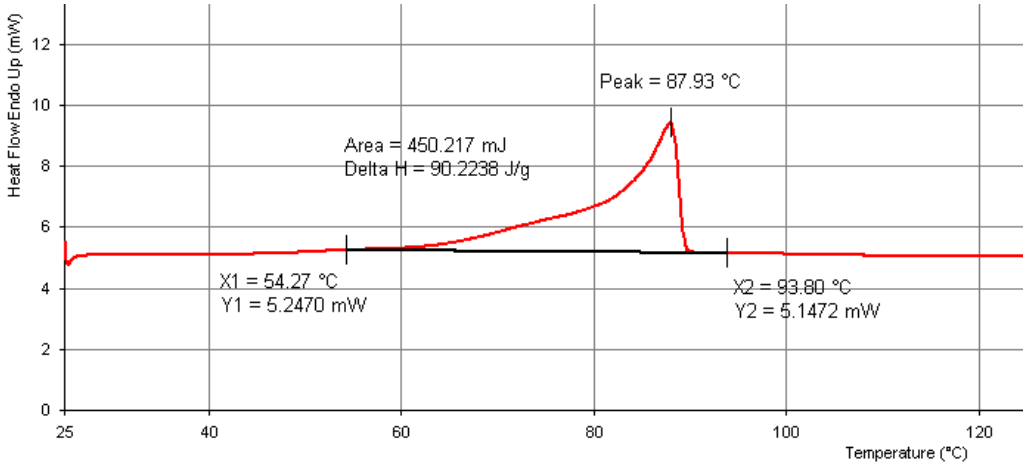

ESI-Fig.4 DSC curve for PIR·LiBr·2H_2O in open pan.

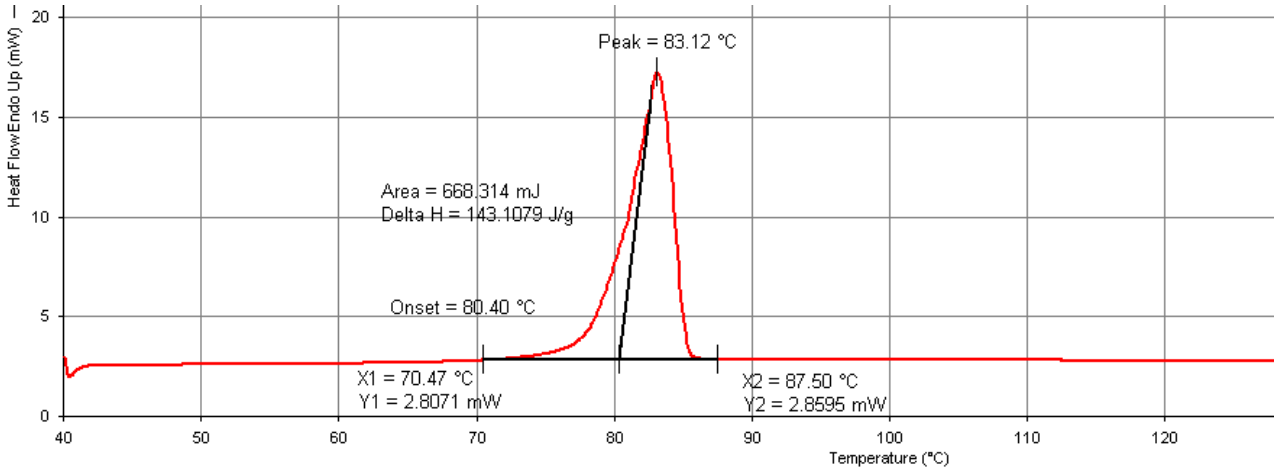

ESI-Fig.5 DSC trace for PIR·LiCl·2H_2O in sealed pan.

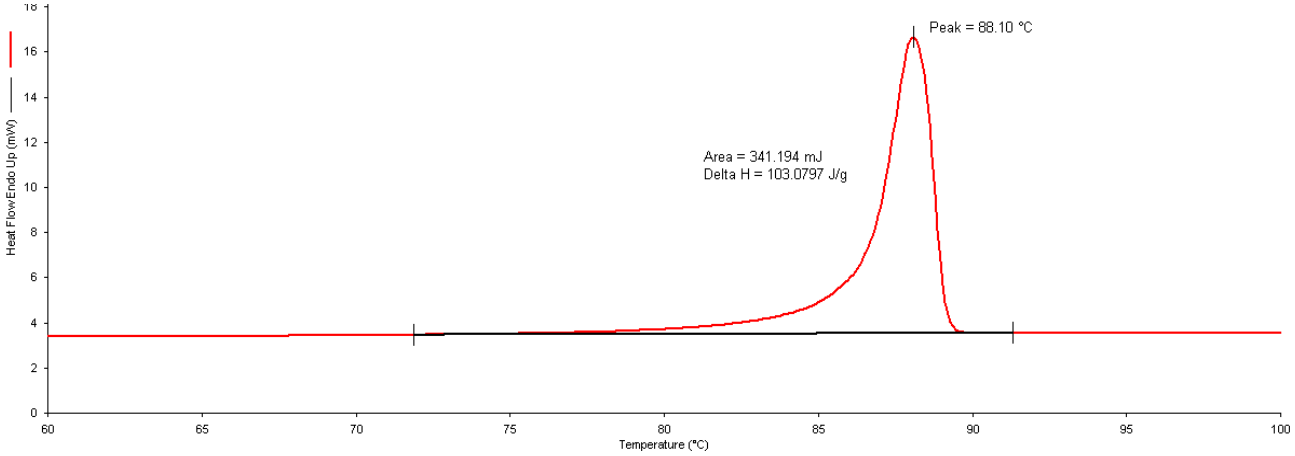

ESI-Fig.6 DSC trace for PIR·LiBr·2H_2O in sealed pan.

X-Ray powder diffraction measurements.

X-ray diffraction patterns were collected on a Panalytical X'Pert PRO automated diffractometer with Cu-Kα radiation and X'Celerator detector without a monocromator, equipped with Anton Paar TTK 450 for measurements at controlled temperature.

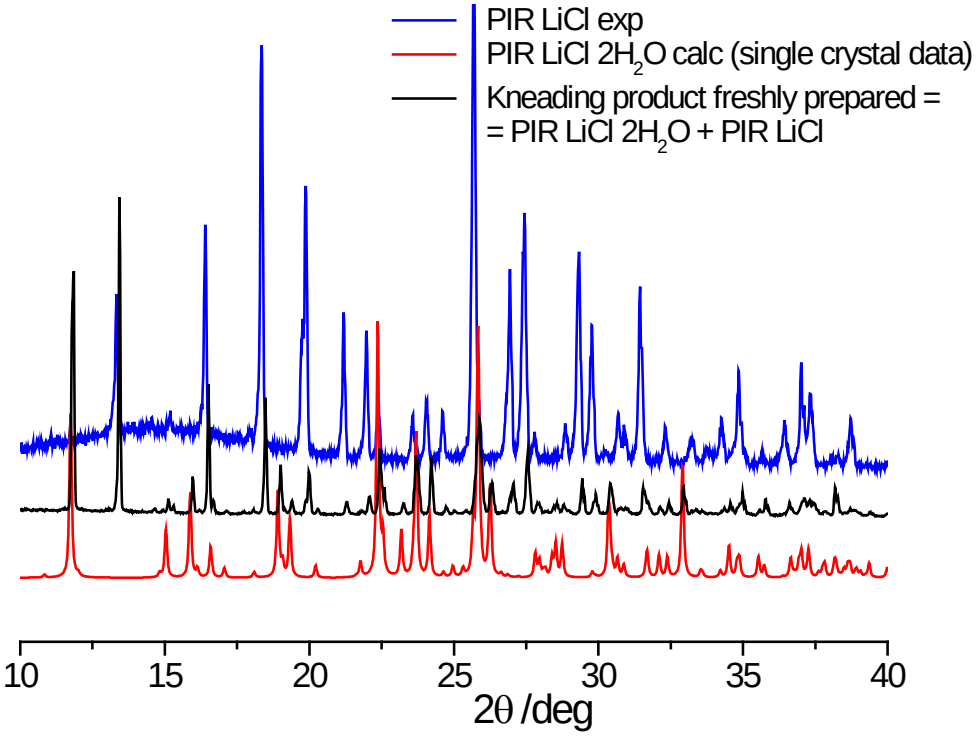

ESI-Fig.7 PIR·LiCl·$2H_2O$: comparison between experimental (black line, product of the kneading process), anhydrous PIR·LiCl (experimental, blue line) and calculated (red line, data from single crystal) X-ray diffraction patterns.

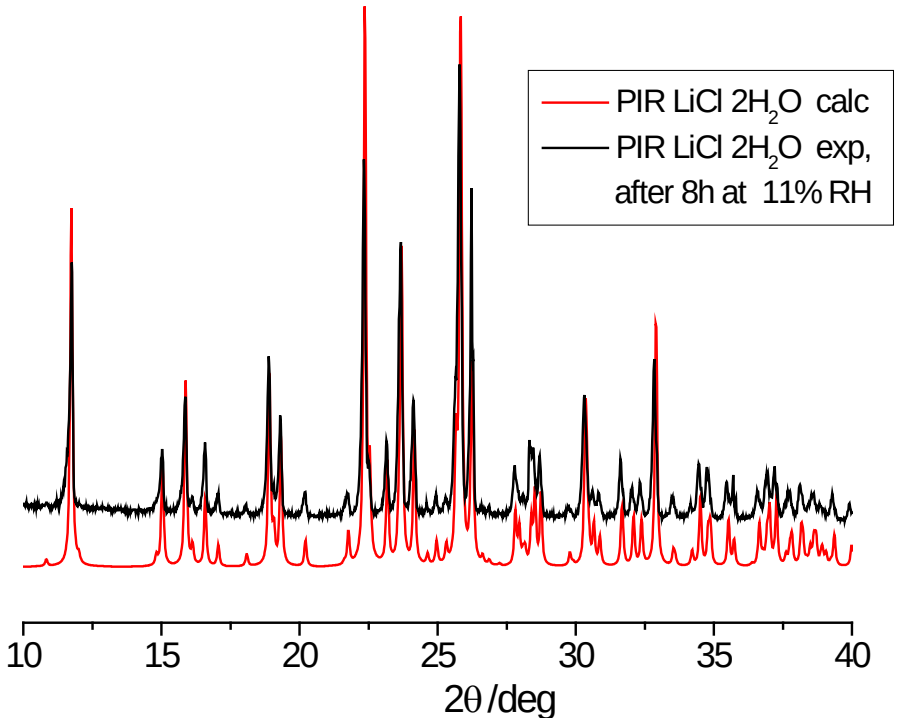

ESI-Fig.8 PIR·LiCl·$2H_2O$: comparison between experimental (black line, product of the kneading process after exposure at 11%RH for 8 hours) and calculated (red line, data from single crystal) X-ray diffraction patterns.

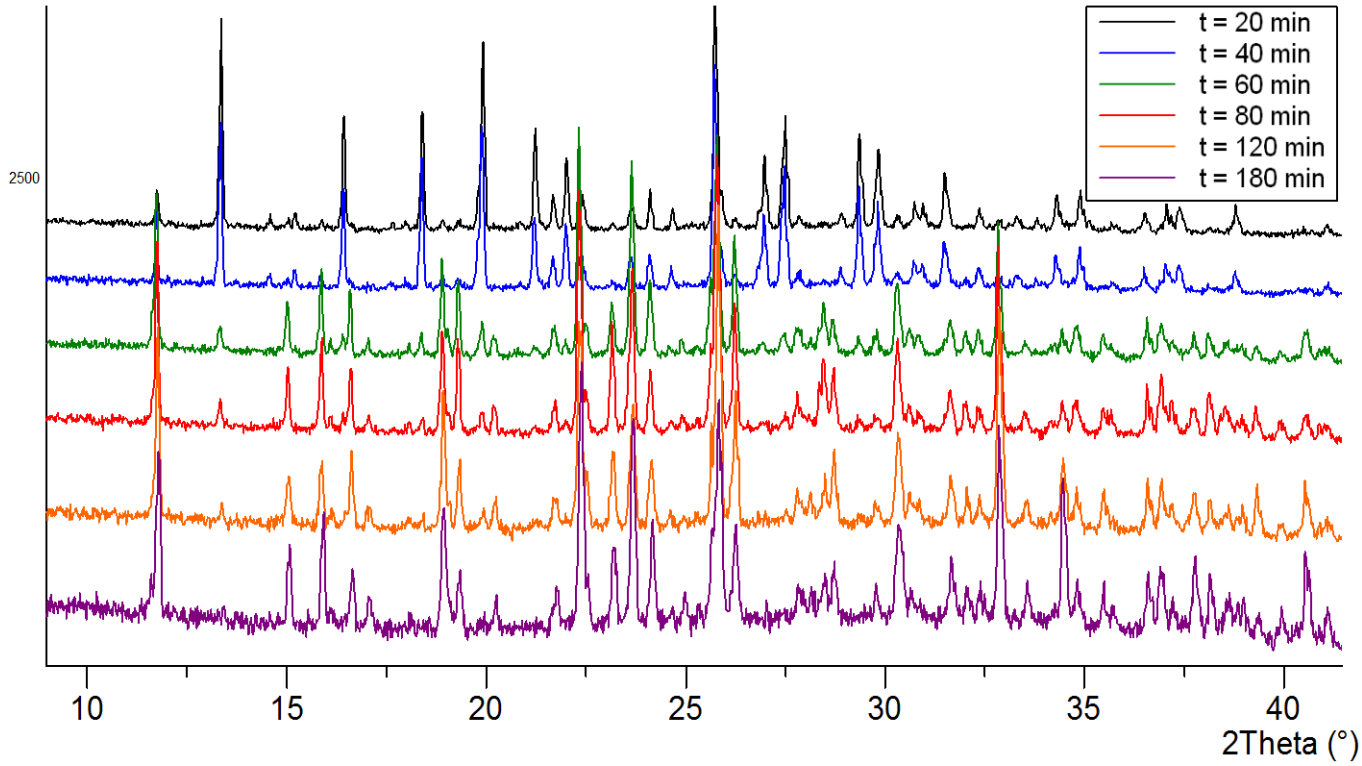

ESI-Fig. 9 Kinetic of rehydration for PIR·LiCl at RT: traces of PIR·LiCl·2H_2O are detectable already after 20 min; after 60 min the hydrated phase PIR·LiCl·2H_2O is the major component, and after 180 min the transformation can be considered complete.

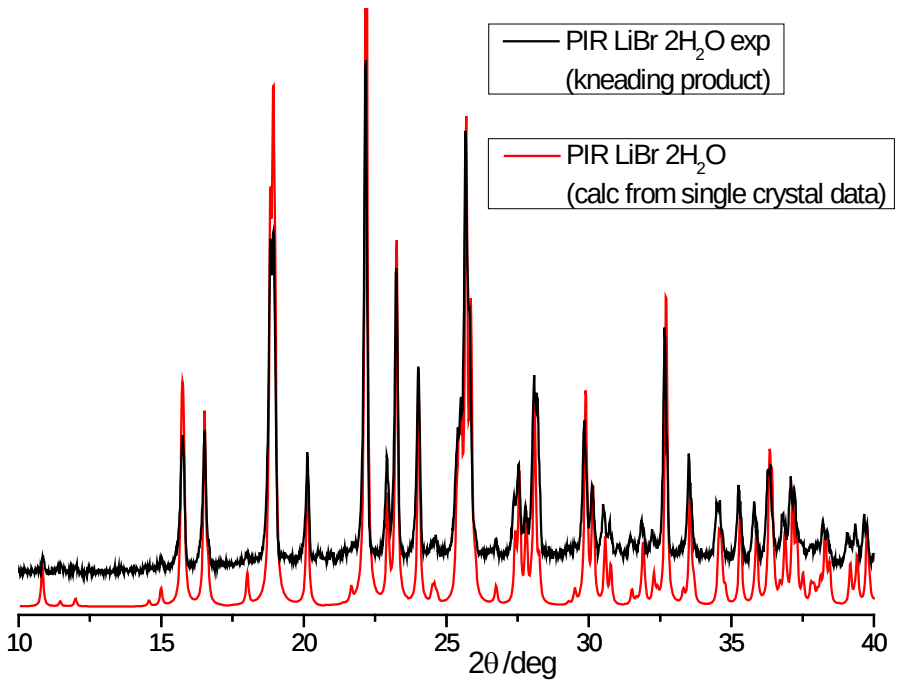

ESI-Fig.10 PIR·LiBr·2H_2O: comparison between the experimental (a, product of the grinding process) and calculated (b, single crystal) X-ray diffraction patterns.

Crystal structure determination from:

1) Single crystal data. All crystal data were collected on an Oxford Xcalibur S with Mo-Kα radiation, λ = 0.71073 Å and monochromator graphite at room temperature. Crystal data and details of measurements are summarized in ESI Table 1. SHELX97[ESI-1] was used for structure solution and refinement based on F^2. Non-hydrogen atoms were refined anisotropically. Hydrogen atoms bound to carbon atoms were added in calculated positions. Hydrogen atoms bound to nitrogen and oxygen atoms were located from a Fourier map and their position refined. In the case of PIR·LiBr·$2H_2O$, constraints were added to water during the refinement, as O-H distances were too short and the H-O-H value could not be kept at reasonable values. Mercury[ESI-2]and Schakal[ESI-3] were used for the graphical representation of the results. The program PLATON[ESI-4] was used to calculate hydrogen bond distances and packing parameters.

2) Powder data.

For structure solution and refinement, an X-ray powder diffractogram in the 2θ range 5–90° (step size, 0.0167°; 0.02 rad soller; kV x mA 40 × 40) was collected in a capillary on a Panalytical X'Pert PRO automated diffractometer equipped with focusing mirror and a Pixel detector. For phase identification, an X-ray powder diffractogram in the 2θ range 5–40° (step size, 0.0167°; 0.04 rad soller; kV x mA 40 × 40) was collected on a Panalytical X'Pert PRO automated diffractometer in Bragg–Brentano geometry equipped with an X'Celerator detector and a variable temperature camera Anton Paar TTK450. All data were collected using Cu Kα radiation without a monochromator.

The powder XRD pattern of PIR·LiCl was indexed using DICVOL04,[5] and the space group assigned as $P2_1/n$ from systematic absences. Unit cell was determined and profile refinement was conducted using the Pawley profile fitting procedure. Refined unit cell and profile parameters were used for structure solution calculations, via direct-space simulated annealing technique implemented in the program DASH.[6] The best structure solution was used as the initial model for Rietveld refinement, which was carried out using the TOPAS program.[7] Final Rietveld refinement (see ESI Fig. 11) resulted in the following parameters: a = 9.1230(1) Å, b = 12.1788(2) Å, c = 8.1089(2) Å, β = 101.8548(8)°; V = 881.743(9) $Å^3$; R_{wp} = 2.92%, R_p = 2.23%.

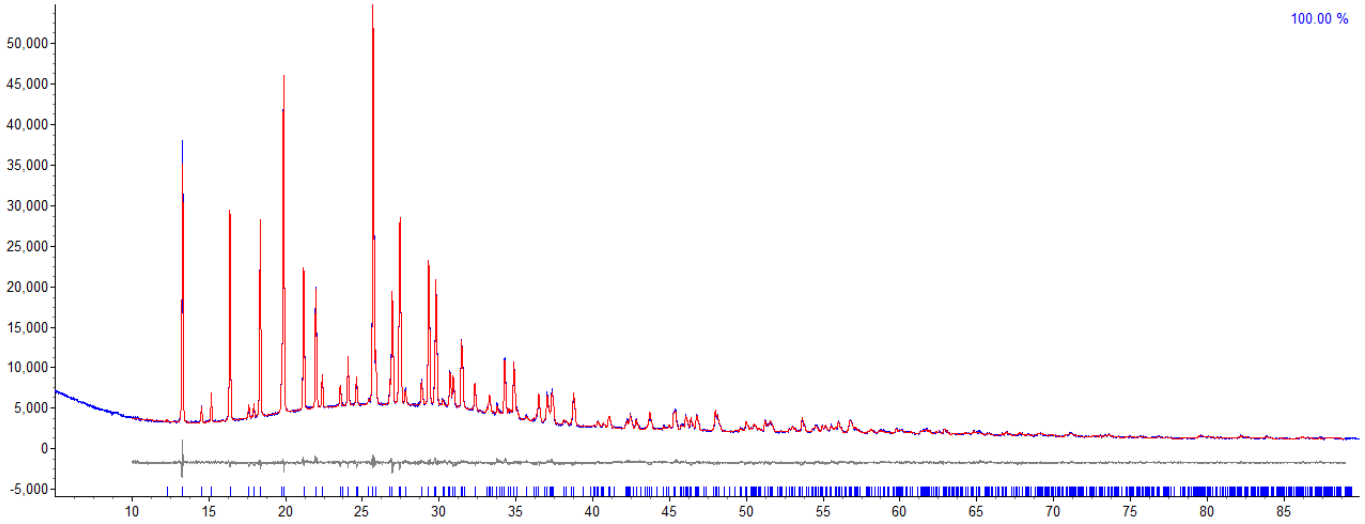

ESI-Fig. 11 Rietveld refinement of PIR LiCl: experimental (blu), calculated (red) and difference (grey) powder X-ray diffraction profiles. Reflection positions are marked.

References

ESI-1 G. M. Sheldrick, *SHELXL97* **1997**, University of Göttingen, Germany.

ESI-2 C. F. Macrae, P. R. Edgington, P. McCabe, E. Pidcock, G. P. Shields, R. Taylor, M. Towler and J. van De Streek, *Journal of Applied Crystallography* **2006**, *39*, 453-457.

ESI-3 E. Keller, **1999**, SCHAKAL99, Graphical Representation of Molecular Models; University of Freiburg, Germany,.

ESI-4 A. L. Spek, *Journal of Applied Crystallography* **2003**, *36*, 7-13.

ESI-5 A. Boultif and D. Louer, *J. Appl. Crystallogr.*, 2004, **37**, 724-731.

ESI-6 W. I. F. David, K. Shankland, J. van de Streek, E. Pidcock, W. D. S. Motherwell and J. C. Cole, *J. Appl. Crystallogr.*, 2006, **39**, 910-915.

ESI-7 A. Coelho, *TOPAS-Academic*, (2007) Coelho Software, Brisbane, Australia.

ESI Table 1. Crystal data and details of measurements for PIR·LiX·2H_2O (X = Cl, Br) and PIR·LiCl

	PIR·LiCl·2H_2O	**PIR·LiCl**	**PIR·LiBr·2H_2O**
Formula	$C_6H_{14}ClLiN_2O_4$	$C_6H_{10}ClLiN_2O_2$	$C_6H_{14}BrLiN_2O_4$
Mol wt	220.58	184.55	265.04
Crystal system	Monoclinic	Monoclinic	Monoclinic
Space group	$P2_1/c$	$P2_1/n$	$P2_1/c$
a (Å)	7.5347(11)	9.1230(1)	7.7723(5)
b (Å)	9.7992(11)	12.1788(2)	9.8812(7)
c (Å)	14.732(3)	8.1089(2)	14.8483(11)
α (°)	90	90	90
β (°)	91.596(13)	101.8548(8)	90.404(6)
γ (°)	90	90	90
V (Å³)	1087.3(3)	881.7	1140.32(14)
Z	4	4	4
Density (g cm^{-3})	1.348	-	1.544
F(000)	464	-	536
μ(MoKα) (mm^{-1})	0.341	-	3.595
Measured reflns	4868	-	6234
Unique reflns	2353	-	2461
Refined parameters	133	-	141
GOF on F^2	0.958	-	1.087
R_1 (onF, I >2s(I)	0.0615	-	0.0488
WR_2 (F^2, all data)	0.1958	-	0.0949

Intrinsic Dissolution Rate (IDR)

Intrinsic dissolution rate was measured only for the hydrated systems, as the anhydrous ICCs are not stable towards humidity.

Measurements were carried out with a Varian Cary 50 Spectrophotometer equipped with a fibre optic dip probe. Five standard solutions in physiological solution (NaCl 0.1 M) at concentrations of 6.25, 12.50, 25.00, 50.00 and 100.00 mg L^{-1} were used to calculate a calibration curve for piracetam (correlation coefficient 0.99583). We analyzed the dissolution rate at room temperature of piracetam (commercial, form III), piracetam$_2$·LiCl·2H$_2$O and piracetam·LiBr·2H$_2$O. We measured the absorbance and used the linear part of the spectrum between 0.1 and 0.5 min, its slope corresponding to the dissolution rate in that interval of time, expressed in Abs min^{-1}. The Abs min^{-1} values were then interpolated in the calibration curve to find the dissolution rate of the analytes expressed as mg $L^{-1}min^{-1}$.

Packing diagrams

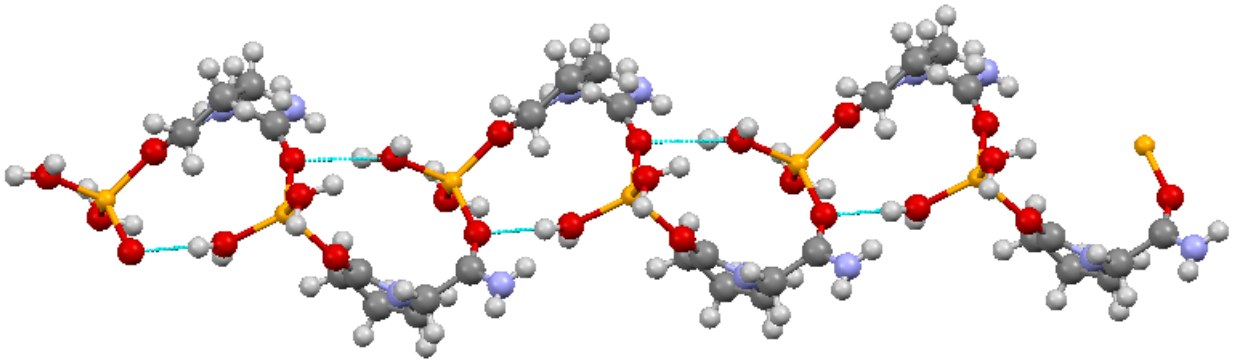

ESI Fig. 10 PIR·LiCl·2H$_2$O : Expanded view of manuscript Fig. 1, top left

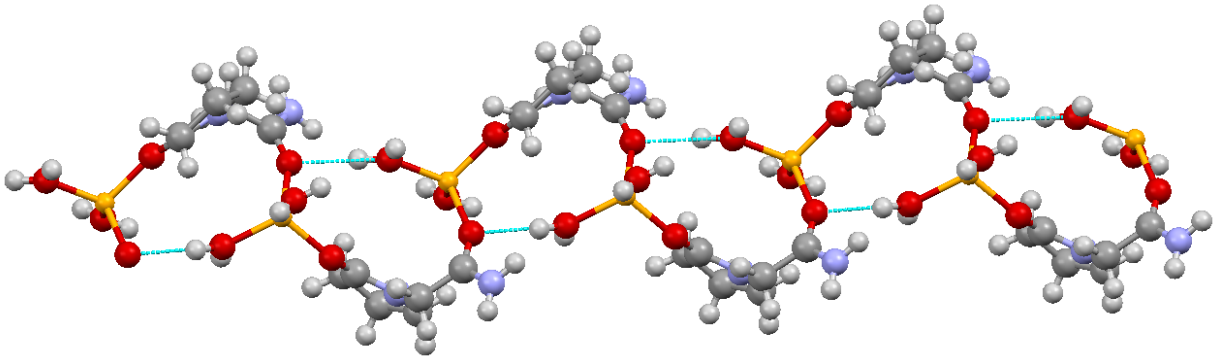

ESI Fig. 11 Same view as in previous figure, for isomorphous PIR·LiBr·2H$_2$O

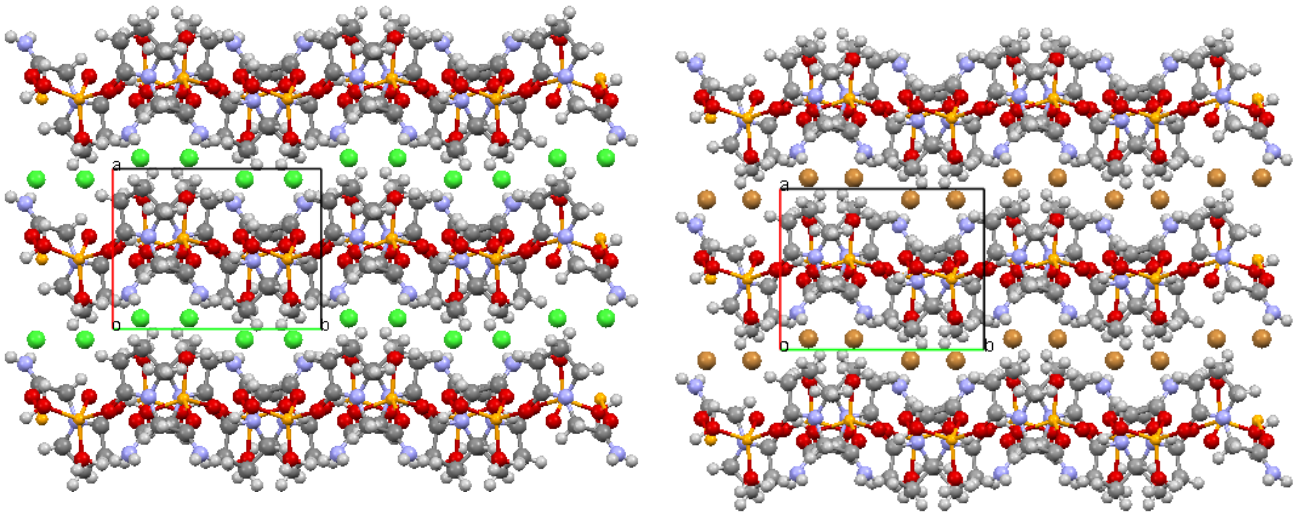

ESI Fig. 12 (left) PIR·LiCl·2H_2O : view down the *c*-axis.; (right) Same view as in previous figure, for isomorphous PIR·LiBr·2H_2O

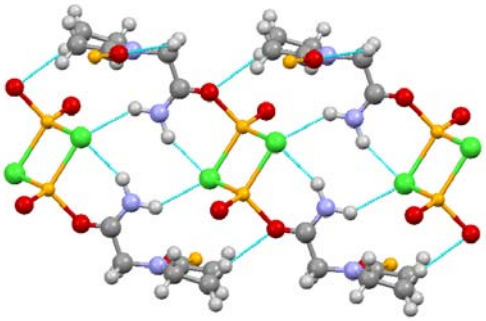

ESI Fig. 13 PIR·LiCl : Expanded view of manuscript Fig. 1, bottom left

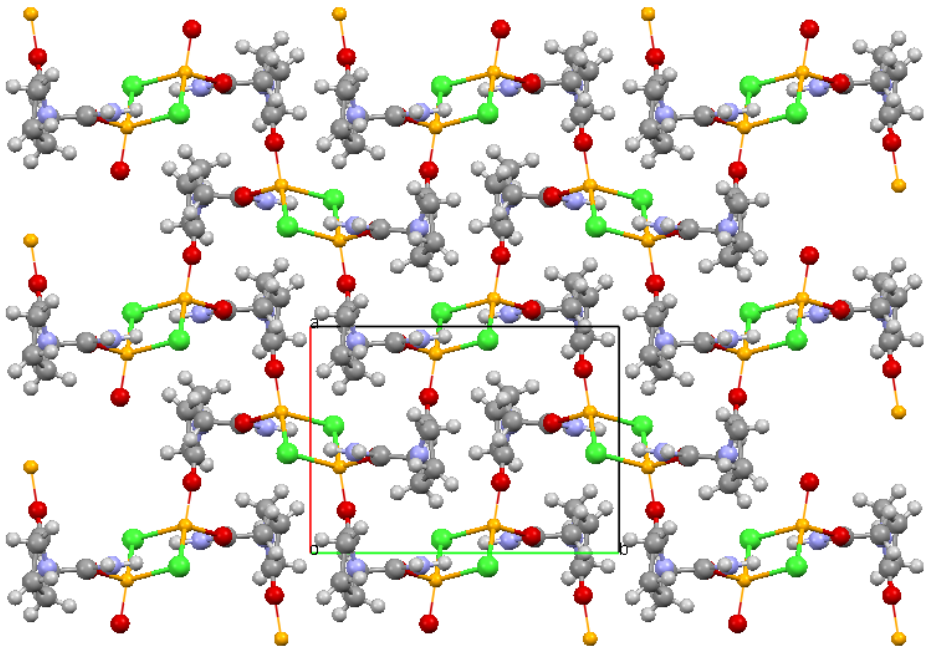

ESI Fig. 14 PIR·LiCl : View down the *c*-axis